Proc. Natl. Acad. Sci. USA
Vol. 90, pp. 9654–9658, October 1993
Neurobiology

Postsynaptic factors in the expression of long-term potentiation (LTP): Increased glutamate receptor binding following LTP induction *in vivo*

(hippocampus/synaptic plasticity/AMPA receptor/NMDA receptor/rat)

STEPHEN MAREN*, GEORGES TOCCO, STEVE STANDLEY, MICHEL BAUDRY, AND RICHARD F. THOMPSON

Neurosciences Program, University of Southern California, Los Angeles, CA 90089-2520

Communicated by William T. Greenough, June 28, 1993 (received for review November 25, 1992)

ABSTRACT **Several lines of evidence indicate that LTP in the hippocampus is associated with a change in the properties of postsynaptic glutamate receptors. In the present study, we used quantitative autoradiography to examine the binding properties of the α-amino-3-hydroxy-5-methyl-4-isoxazole-propionate (AMPA) and *N*-methyl-D-aspartate subclasses of glutamate receptors in frozen brain sections obtained from rats in which perforant-path LTP was induced *in vivo*. Induction of LTP resulted in a selective increase in [^{3}H]AMPA binding in those hippocampal subfields receiving perforant-path axons. Increases in [^{3}H]AMPA binding in dentate gyrus (stratum moleculare) were highly correlated with the magnitude of LTP recorded in this structure. Scatchard analyses of [^{3}H]AMPA and 6-cyano-7-nitro-[^{3}H]quinoxaline-2,3-dione (an AMPA receptor antagonist) binding in the dentate gyrus indicated that LTP induction resulted in an increase in the number of AMPA receptor binding sites. No changes in the binding of ^{3}H-labeled *N*-[1-(thienyl)cyclohexyl]piperidine (an *N*-methyl-D-aspartate receptor antagonist) were observed in any hippocampal subfield. These results suggest that a modification in postsynaptic AMPA receptors plays a role in the expression of synaptic enhancement following LTP induction in the hippocampus.**

LTP of excitatory synaptic transmission in the hippocampus is an enduring form of synaptic enhancement that may underlie some forms of mammalian learning and memory (1, 2). While consensus has been reached on the cellular mechanisms involved in triggering LTP, the nature of the persistent synaptic modification underlying the expression of LTP is still a matter of debate (3). There is a growing body of evidence that LTP is expressed, at least in part, by a persistent modification of postsynaptic α-amino-3-hydroxy-5-methyl-4-isoxazolepropionate (AMPA) receptors, a subclass of ionotropic glutamate receptors (4–9). This modification may be variously expressed as an increase in the binding affinity of AMPA receptors, an increase in the number of AMPA binding sites, or a change in the kinetics of AMPA receptor-gated ion channels. To further restrict these possibilities, we have examined the binding properties of postsynaptic AMPA and *N*-methyl-D-aspartate (NMDA) receptors (another subclass of ionotropic glutamate receptors) in frozen brain sections following perforant-path LTP induction *in vivo*. We report a selective increase in hippocampal AMPA receptor binding following perforant-path LTP induction that is apparently mediated by an increase in the number of AMPA binding sites. These results suggest that a change in the binding properties of AMPA receptors contributes to the enhanced synaptic transmission observed at hippocampal synapses following LTP induction.

The publication costs of this article were defrayed in part by page charge payment. This article must therefore be hereby marked "*advertisement*" in accordance with 18 U.S.C. §1734 solely to indicate this fact.

MATERIALS AND METHODS

Subjects and Surgery. Adult male Long–Evans rats (250–300 g) were anesthetized with an i.p. injection of sodium pentobarbital (65 mg/kg) and implanted with a recording electrode in the hilus of the dentate gyrus and a bipolar stimulating electrode in the perforant path (9). The electrodes consisted of Epoxylite-coated stainless-steel pins with the recording and stimulating surfaces formed by removing the insulation at the tips. The electrode tip lengths were 50 and 500 μm for recording and stimulating electrodes, respectively.

Acute Electrophysiology. All electrophysiological testing was performed under surgical anesthesia. Extracellular field potentials evoked by single-pulse perforant-path stimulation pulses (0.1 msec, 0.05 Hz) were recorded in the dentate gyrus during a 10-min interval before and a 60-min interval following high- or low-frequency perforant-path stimulation (HFS or LFS). Fig. 1*A* represents the perforant-path stimulation parameters used to induce LTP. Subjects in HFS groups received either 20 (HF-20, $n = 6$), 100 (HF-100, $n = 6$), or 200 (HF-200, $n = 6$) pulses using the patterns in Fig. 1*A*. Six animals served as controls for nonspecific effects of intracranial brain stimulation and received LFS (1 Hz for 200 sec; 200 pulses). These groups allowed us to examine the effects of both the quantity and pattern of HFS on hippocampal LTP and glutamate receptor binding. Data from the HF-200 animals were as reported (10). Current intensities were adjusted to elicit a 1- to 2-mV population spike (PS) in all subjects.

Binding Assays. One hour after HFS or LFS, the rats were decapitated and their brains were rapidly removed, frozen in −20°C isopentane, and stored at −70°C until sectioning. Frozen coronal sections (10 μm) cut at or near the hilus recording site were used for all assays; each assay was performed on at least four sections from each animal. For binding of [^{3}H]AMPA (55.6 Ci/mmol; NEN; 1 Ci = 37 GBq), slides were equilibrated to room temperature and preincubated for 30 min at 35°C in 100 mM Tris acetate, pH 7.4/100 mM KSCN/100 μM EGTA. Sections were then incubated at 0–4°C for 45 min in the same buffer containing 150 nM [^{3}H]AMPA with or without 1 mM quisqualate (to determine nonspecific binding). After incubation, slides were rinsed at 0–4°C twice (10 sec per rinse) in 100% buffer and once (5 sec) in 50% buffer, dipped three times in distilled water, and rapidly dried under a stream of warm air. Nonspecific binding

Abbreviations: AMPA, α-amino-3-hydroxy-5-methyl-4-isoxazole-propionate; CNQX, 6-cyano-7-nitroquinoxaline-2,3-dione; TCP, *N*-[1-(thienyl)cyclohexyl]piperidine; NMDA, *N*-methyl-D-aspartate; LTP, long-term potentiation; EPSP, excitatory postsynaptic potential; PS, population spike; HFS, high-frequency perforant-path stimulation; LFS, low-frequency perforant-path stimulation; DGmol, dentate gyrus stratum moleculare; CA1rad and CA3rad, stratum radiatum/lacunosum–moleculare of hippocampal regions CA1 and CA3; CA1or and CA3or, stratum oriens of CA1 and CA3.

*To whom reprint requests should be addressed at: Department of Psychology, University of California, Los Angeles, CA 90024-1563.

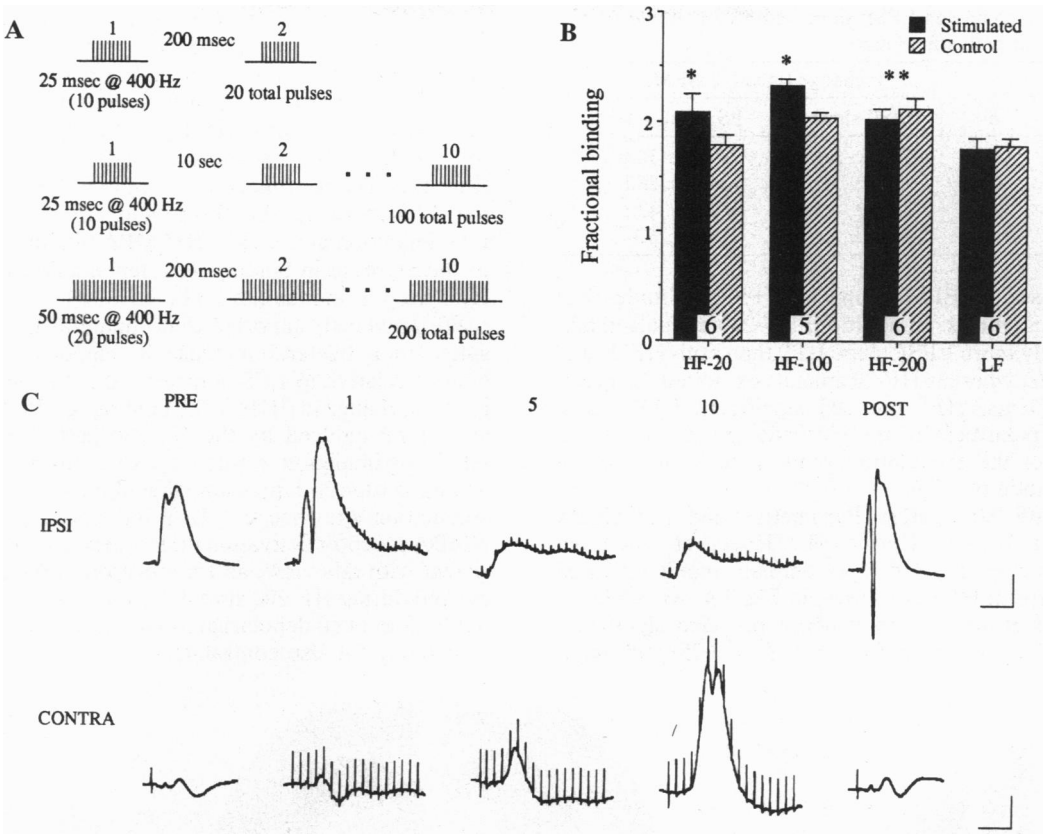

FIG. 1. (*A*) HFS parameters. Low-frequency controls received 200 pulses at 1 Hz. All perforant-path stimulation was unilateral, and the unstimulated hemisphere served as a within-subject control. (*B*) Mean fractional AMPA binding (±SEM) in dentate gyrus stratum moleculare (DGmol) for the groups described in *A*. Data are represented as a fraction of ipsilateral cerebral cortical binding; the number of rats in each group is shown in the bars. Single asterisks indicate a significant lateralization of binding in the HF-20 and HF-100 groups, and the double asterisks indicate a significant difference between the HF-200 and LF groups. (*C*) Extracellular perforant-path-evoked field potentials recorded in the hilus of the dentate gyrus ipsilateral (IPSI) and contralateral (CONTRA) to the stimulation site in an HF-200 animal. PRE and POST potentials are averages of 20 responses evoked during the 10-min intervals immediately before and 50–60 min after HFS. Ipsilateral field potentials consisted of a positive-going population excitatory postsynaptic potential (EPSP) with a sharp, negative-going PS superimposed upon it, whereas contralateral field potentials consisted of a small-amplitude monosynaptic response, followed by a larger-amplitude disynaptic response (onset latency ≈ 10 msec). The three interposed potentials were recorded during the 1st, 5th, and 10th bursts of the 10-burst HF-200 stimulation train. Note the incremental depolarization in the contralateral hemisphere during the stimulation train and the consequent potentiation of the commissural response. Calibration: 10 msec, 5 mV (IPSI) or 500 μV (CONTRA).

represented <10% of the total binding. [^{3}H]CNQX (6-cyano-7-nitroquinoxaline-2,3-dione, an AMPA receptor antagonist; 29.2 Ci/mmol; NEN) binding was assessed with the same procedures used for AMPA binding except that 100 μM glycine was included in the incubation to inhibit CNQX binding to the glycine site on the NMDA receptor. The concentration of [^{3}H]CNQX was 75 nM and KSCN was not included in the incubation. In additional assays, saturation curves for [^{3}H]AMPA and [^{3}H]CNQX binding were generated by using five concentrations of each ligand (AMPA at 22, 66, 500, 1000, and 2000 nM; CNQX at 11, 33, 100, 400, and 1000 nM). Alternate pairs of slides (four brain sections per slide) were used for each ligand and concentration. For [^{3}H]TCP {*N*-[1-(thienyl)cyclohexyl]piperidine, an NMDA receptor antagonist; 47.8 Ci/mmol; NEN} binding, slides were equilibrated to room temperature and preincubated at 35°C for 30 min in 100 mM Hepes, pH 7.4/50 μM EGTA/10 μM glutamate/10 μM glycine. Sections were then incubated for 45 min at room temperature in the same buffer containing 100 nM [^{3}H]TCP with or without 5 mM ketamine (to determine nonspecific binding). The slides were rinsed and dried as for AMPA binding, except that the rinses were performed at room temperature. Nonspecific binding represented <15% of the total binding.

Autoradiographic film (HyperFilm; Amersham) was pressed against the tissue sections and radioactive standards. After exposure for 10–15 days, the films were developed for 3–5 min at room temperature in Kodak GBX developer and fixer. Autoradiographs were analyzed to determine the amount of ligand binding in five hippocampal subfields: DGmol, stratum radiatum/lacunosum–moleculare (CA1rad, CA3rad), and stratum oriens (CA1or, CA3or). In addition, binding in the thalamus and cerebral cortex overlying the dorsal hippocampus was quantified. Optical density measurements were made in each hemisphere, averaged across replicate sections, and transformed to specific binding. For statistical analysis, a "fractional binding" index was adopted. It consisted of the ratio of specific binding in hippocampal or thalamic regions to that in the overlying cortex, and served to reduce the within- and between-section variability in binding.

RESULTS

Perforant-Path Stimulation Parameters and LTP in the Dentate Gyrus. Table 1 shows the mean percent changes in population EPSP slope and PS amplitude 1 hr after HFS or LFS. Analysis of variance (ANOVA) revealed significant group differences in the percent change of both EPSP slope [$F(3, 18) = 16.5$, $P < 0.01$] and PS amplitude [$F(3, 18) = 13.0$, $P < 0.01$]. Post-hoc comparisons (Fisher tests, $P < 0.05$) indicated that all of the HFS groups showed significantly

Table 1. Percent change in EPSP slope and PS amplitude following perforant-path stimulation

Group	*n*	% change (mean ± SEM) EPSP slope	PS amplitude
HF-20	6	12.0 ± 1.1	299.7 ± 32.0
HF-100	5	9.6 ± 3.2	134.7 ± 26.8
HF-200	6	27.7 ± 4.4	170.7 ± 42.5
LF	6	−2.9 ± 2.6	21.2 ± 6.1

greater increases in EPSP slope and PS amplitude than low-frequency controls. In addition, HF-200 animals exhibited significantly more EPSP slope LTP than both HF-20 and HF-100 animals, whereas HF-20 animals exhibited the greatest PS LTP. Thus, HFS induced significant LTP in the dentate gyrus regardless of the particular pattern of stimulation, although the stimulation pattern did influence the relative magnitude of LTP.

Perforant-Path Stimulation Parameters and [^{3}H]AMPA Binding in the Dentate Gyrus. The levels of fractional [^{3}H]AMPA binding in DGmol of animals receiving three different patterns of HFS are shown in Fig. 1*A*. An ANOVA with factors of group and hemisphere revealed significant main effects of group [$F(3, 19) = 3.4$, $P < 0.05$] and hemisphere [$F(1, 19) = 7.8$, $P < 0.05$], as well as a significant interaction of the two [$F(3, 19) = 5.5$, $P < 0.01$]. Post-hoc comparisons (Fisher tests, $P < 0.05$) indicated that the HF-20 and HF-100 patterns of stimulation produced lateralized increases in [^{3}H]AMPA binding in the dentate gyrus, whereas the HF-200 pattern induced a bilateral increase in binding (Fig. 1*B*). The lateralized increase in [^{3}H]AMPA binding did not differ between the HF-20 and HF-100 groups. Hence, LTP induction increased [^{3}H]AMPA binding, and the nature of the increase in binding was dependent on the pattern of HFS used to induce the LTP.

We previously reported that unilateral HFS (HF-200) resulted in a bilateral increase in hippocampal [^{3}H]AMPA binding relative to LFS controls (10). It is possible that this bilateral change in [^{3}H]AMPA binding resulted from polysynaptic LTP induced by the HF-200 pattern of HFS. If so, HF-200 stimulation would be expected to produce strong depolarization in hippocampal subfields contralateral to the stimulation site, because LTP induction typically requires NMDA receptor activation under these conditions (11). Consistent with this view, an examination of the field potentials evoked during HF-200 stimulation ($n = 4$) revealed substantial HFS-evoked depolarization in the dentate gyrus not only ipsilateral, but also contralateral to the perforant-path stim-

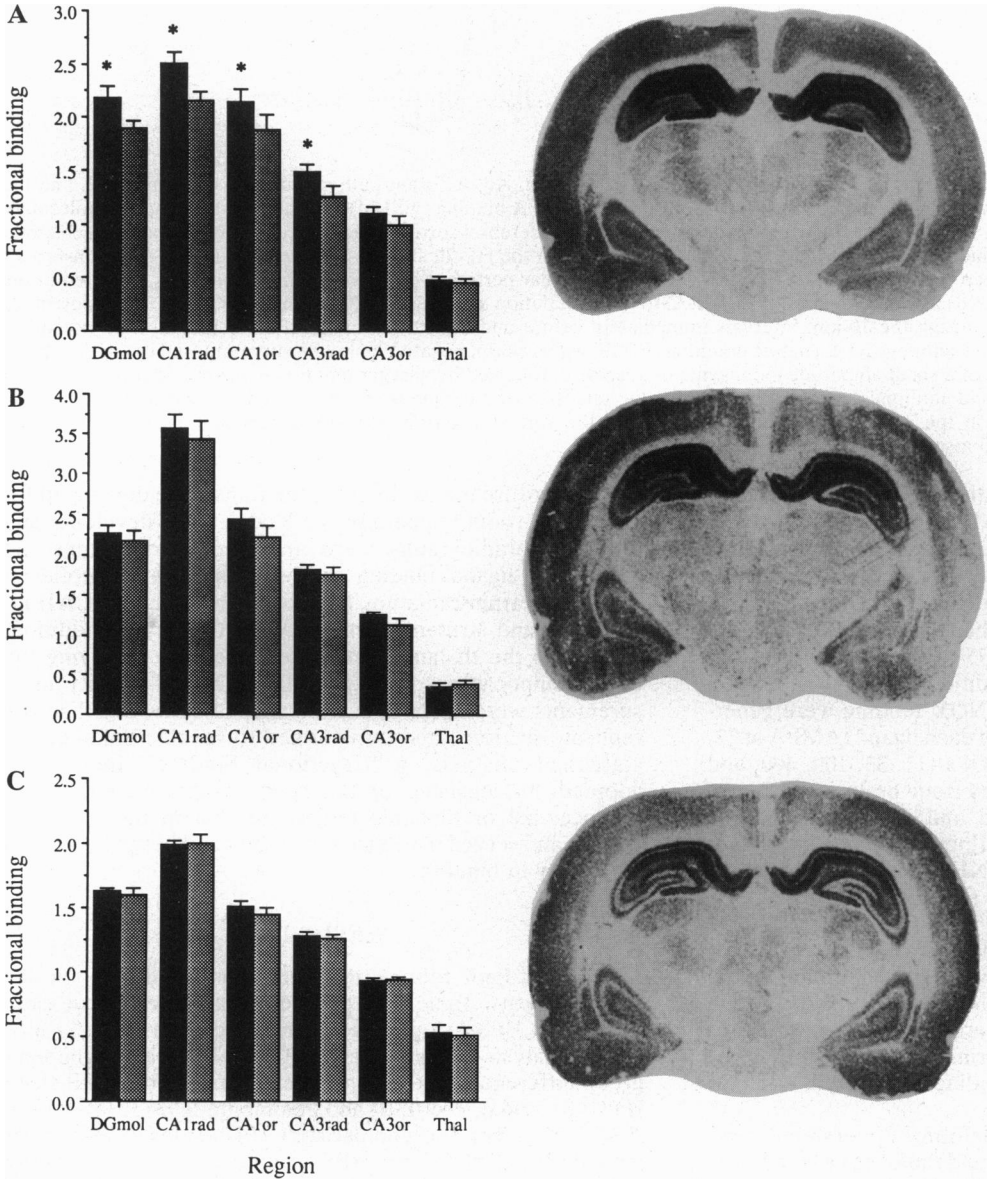

FIG. 2. [^{3}H]AMPA (*A*), [^{3}H]-CNQX (*B*), and [^{3}H]TCP (*C*) binding in six brain regions 1 hr after perforant-path LTP induction. Solid bars, fractional binding in the stimulated (potentiated) hemisphere; stippled bars, fractional binding in the unstimulated (control) hemisphere. Binding data (means ± SEMs) are represented as a fraction of ipsilateral cerebral cortical binding. Eleven rats (HF-20 and HF-100 groups) were used in each binding experiment. Asterisks indicate significant increases in AMPA binding in hippocampal regions of the stimulated hemisphere. No changes in either [^{3}H]CNQX or [^{3}H]TCP binding were evident in any brain region. Representative autoradiographs are shown next to the bar graphs; the left hemisphere (i.e., the left side of the autoradiograph) received HFS. Thal, thalamus.

ulation site (Fig. 1*C*). The contralateral depolarization during HFS was polysynaptic (latency ≈10 msec, consistent with a disynaptic pathway) and incremental (i.e., it markedly increased in magnitude during HFS). Moreover, although different in form from that in the ipsilateral dentate gyrus, it also resulted in LTP (e.g., compare PRE and POST responses in Fig. 1*C*). This was apparent in all four animals tested under these conditions. In contrast, neither the HF-20 nor the HF-100 patterns of HFS were associated with commissural depolarization or polysynaptic LTP (data not shown). Insofar as the enhancement of the commissural response reflects LTP in the contralateral dentate gyrus, it is possible that the HF-200 pattern of perforant-path stimulation produced "transsynaptic" LTP in several hippocampal subfields (see ref. 12 for a similar report). This could account for the contralateral changes in hippocampal [^{3}H]AMPA binding observed in HF-200 subjects.

Regional Distribution of [^{3}H]AMPA Binding and Perforant-Path LTP. The regional distribution of AMPA receptor binding in the HF-200 group has been described elsewhere (10) and will not be considered here. In addition, there were no significant differences between the HF-20 and HF-100 groups in either receptor binding or physiology, so they were combined for subsequent analyses. [^{3}H]AMPA binding to a coronal brain section from a representative subject is shown in Fig. 2*A*. Hippocampal LTP induction using patterns of HFS not associated with commissural depolarization resulted in a significant lateralized increase in [^{3}H]AMPA binding in a number of brain regions [$F(5, 50) = 5.9$, $P < 0.01$]. As shown in Fig. 2*A*, post-hoc comparisons (Fisher tests, $P < 0.05$) identified significant increases in [^{3}H]AMPA binding in DGmol, CA1rad, CA1or, and CA3rad in the potentiated hemisphere compared with the control hemisphere. The relative increase in AMPA binding in DGmol was highly correlated with the amount of LTP recorded in the hilus 1 hr after LTP induction [Fig. 3; $r = 0.93$, $t(10) = 7.6$, $P < 0.01$]. These results indicate that increases in [^{3}H]AMPA binding following HFS are not restricted to the dentate gyrus but also occur in other hippocampal subfields receiving perforant-path axons.

Characterization of Increased AMPA Receptor Binding with Perforant-Path LTP. The increases in hippocampal [^{3}H]AMPA binding produced by HFS could have been due to an increase in either binding affinity or the number of binding sites. Because manipulations that modify AMPA receptor affinity are frequently associated with a decrease in [^{3}H]-CNQX binding, and because increases in AMPA receptor number are reflected by similar increases in both [^{3}H]AMPA and [^{3}H]CNQX binding (13, 14), we examined [^{3}H]CNQX binding as a first step in addressing the nature of the change in AMPA receptors. [^{3}H]CNQX binding showed no significant differences between the HF-20 and HF-100 groups, so they were combined for the subsequent analysis. A representative autoradiograph of [^{3}H]CNQX binding is shown in Fig. 2*B*. In contrast to [^{3}H]AMPA binding, significant lateralization of [^{3}H]CNQX binding was not observed in any brain region [$F(5, 50) = 1.0$, $P = 0.45$; Fig. 2*B*]. However, there was a nonsignificant trend toward increased hippocampal [^{3}H]CNQX binding in the potentiated hemisphere, which is suggestive of an increase in AMPA receptor number following LTP induction.

To examine this issue further, we analyzed the saturation kinetics of [^{3}H]AMPA and [^{3}H]CNQX binding in three HF-20 rats that showed above-average LTP. The saturation curves for [^{3}H]AMPA and [^{3}H]CNQX binding in DGmol are shown in Fig. 4. Scatchard analysis indicated that AMPA receptor densities in the dentate gyrus were elevated with perforant-path LTP (Table 2). Specifically, the number of sites (B_{max}) for both [^{3}H]AMPA [$t(2) = 17.3$, $P < 0.01$] and [^{3}H]CNQX [$t(2) = 4.6$, $P < 0.05$] binding was significantly greater in the potentiated hemisphere. There were no hemispheric differences in receptor affinity (K_d) for either [^{3}H]AMPA [$t(2) = 1.4$, $P = 0.30$] or [^{3}H]CNQX [$t(2) = 0.9$, $P = 0.46$] binding.

Regional Distribution of [^{3}H]TCP Binding and Perforant-Path LTP. Recent evidence indicates that LTP induction does not modify the properties of NMDA receptors under the conditions used in the present study (9). Nevertheless, we

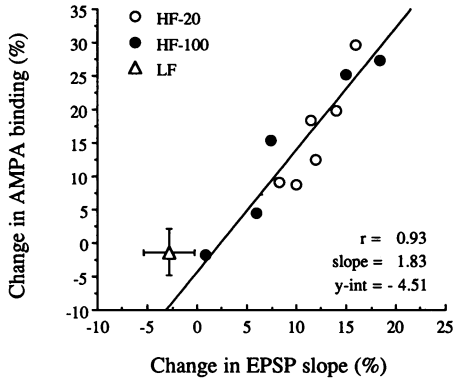

FIG. 3. Relationship between [^{3}H]AMPA binding in DGmol and EPSP-slope LTP in the hilus. Data points are from subjects in the HF-20 (○) and HF-100 (●) groups; data (mean ± SEM) from animals that received LFS (△) are shown for comparison. Binding values were calculated as the percent change in fractional binding in the stimulated relative to the unstimulated hemisphere. LTP was assessed 1 hr after HFS. The regression line computed for HFS group revealed a Pearson correlation coefficient of 0.93. The slope and *y* intercept of the regression line were 1.83 and −4.51, respectively.

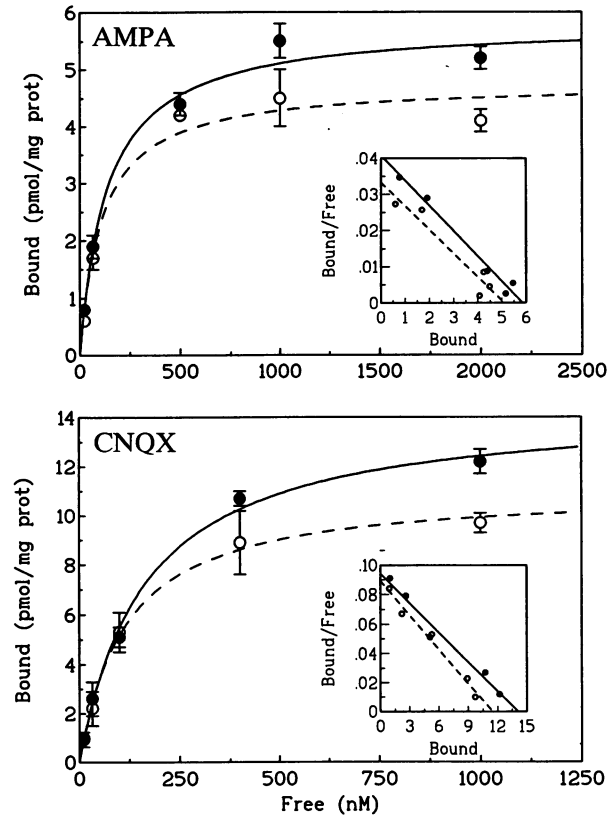

FIG. 4. Saturation kinetics for [^{3}H]AMPA and [^{3}H]CNQX binding in DGmol. ●, Binding in the potentiated hemisphere; ○, binding in the control hemisphere. Saturation curves were generated from five concentrations of each ligand by using tissue from three rats in the HF-20 group. Scatchard analyses (*Insets*) revealed significant increases in B_{max} for both [^{3}H]AMPA and [^{3}H]CNQX binding; no changes in K_d were evident. prot, Protein.

Table 2. Saturation analysis parameters (mean ± SEM) for [^{3}H]AMPA and [^{3}H]CNQX binding in DGmol following perforant-path LTP induction

Parameter	Potentiated	Control
[^{3}H]AMPA		
B_{max}, pmol/mg	5.9 ± 0.3	4.9 ± 0.3
K_d, nM	149.7 ± 23.4	125.9 ± 14.8
[^{3}H]CNQX		
B_{max}, pmol/mg	14.5 ± 0.3	11.2 ± 0.4
K_d, nM	167.1 ± 15.0	131.2 ± 43.8

examined [^{3}H]TCP binding in HF-20 and HF-100 animals to assess the binding properties of NMDA receptors following LTP induction. There were no significant differences between the groups, so they were combined for the subsequent analysis. At saturating concentrations of ligand, no changes in [^{3}H]TCP binding were detected in any brain region [$F(5, 50) = 1.4$, $P = 0.25$; Fig. 2*C*]. This indicates that LTP-related changes in glutamate receptor binding are specific to AMPA receptors.

DISCUSSION

The results indicate that perforant-path LTP induction *in vivo* produces a persistent and selective modification in the binding properties of hippocampal AMPA receptors. Lateralized increases in hippocampal [^{3}H]AMPA binding were observed with patterns of HFS that did not generate commissural depolarization or polysynaptic LTP. These increases in [^{3}H]AMPA binding were most prominent in DGmol, CA1rad, and CA3rad, and the increase in DGmol was highly correlated with the magnitude of LTP recorded in the hilus 1 hr after LTP induction. Saturation analyses indicated that the changes in [^{3}H]AMPA binding produced by LTP induction were due to increases in the number of AMPA receptors. In none of the treatment groups was LTP associated with a change in saturated [^{3}H]TCP binding, suggesting that LTP is not accompanied by a change in the density of NMDA receptors.

The increase in [^{3}H]AMPA binding in CA1 and CA3 with HFS is consistent with an emerging body of evidence that entorhinal cortical axons are capable of strongly exciting hippocampal pyramidal cells both mono- and polysynaptically (15). Accordingly, HFS induces LTP in monosynaptic perforant-path projections to areas CA1 and CA3 (16) and transsynaptic potentiation within the trisynaptic circuitry (12). One or both of these forms of synaptic plasticity may have contributed to the increased [^{3}H]AMPA binding we observed in CA1 and CA3. Similarly, changes in [^{3}H]AMPA binding in hippocampal regions contralateral to HFS may have been due to a combination of mono- and polysynaptic LTP, although the types of pathways involved remain to be determined. Whatever the case may be, the increases in hippocampal [^{3}H]AMPA binding do not appear to be solely the result of HFS-evoked depolarization, because supramaximal HFS yields neither LTP nor changes in [^{3}H]AMPA binding (10). Rather, the increases in [^{3}H]AMPA binding appear to be associated with an LTP-like process, because they only occur following LTP induction and are dependent on NMDA receptor activation (10).

Scatchard analyses revealed increases in [^{3}H]AMPA and [^{3}H]CNQX binding that were apparently due to an increase in the number, not the affinity, of AMPA receptors. Several possibilities could account for these results. First, the analysis of saturation kinetics is more sensitive to small changes in B_{max} than to small changes in K_d, especially when performed with quantitative autoradiography. Therefore, we cannot categorically dismiss the possibility that changes in AMPA receptor affinity accompanied changes in B_{max} or that LTP is associated with a change in the affinity of yet unidentified AMPA receptor states. Indeed, both of these changes might appear as an apparent increase in the number of binding sites. Second, AMPA receptors exist in at least two interconvertible affinity states (13). Our autoradiographic data did not allow a clear distinction between the high- and low-affinity states, and the K_d we measured for [^{3}H]AMPA was intermediate with respect to the values typically reported for the two states. Thus, we cannot be certain whether the observed changes in B_{max} were associated with the high- or low-affinity state. However, recent evidence indicates that, under the conditions used in our experiments, [^{3}H]AMPA binds primarily to low-affinity receptors localized at synaptic sites (S.S., unpublished data). The synaptic localization of low-affinity AMPA receptors is also suggested by the predominance of these receptors in solubilized membrane fractions (17). Based on this evidence, it is reasonable to suggest that our saturation data reflect an increase in the number of low-affinity AMPA receptors.

In conclusion, these data, together with those reported previously (4–10), suggest that a selective change in the properties of postsynaptic AMPA receptors plays a role in the expression of hippocampal LTP *in vivo*. Although we have not examined the time course of changes in [^{3}H]AMPA binding following LTP induction, recent data indicate that similar changes in [^{3}H]AMPA binding persist for at least 24 hr following HFS in awake, behaving animals (18). Together, these findings fit well with the large number of studies indicating that LTP is associated with a change in the properties of postsynaptic AMPA receptors and provide a plausible mechanism for the expression of long-term changes in hippocampal synaptic efficacy.

This work was supported by grants from the National Science Foundation (BNS 911037) and the Office of Naval Research (N00014-91-J-1796) to M.B., by grants from the National Institutes of Health (AG01542), the National Science Foundation (BNS 8718300), the Office of Naval Research (N00014-88-K-0112), and the McKnight Foundation to R.F.T., and by a University of Southern California Dean's Fellowship to S.M.

1. Bliss, T. V. P. & Lømo, T. (1973) *J. Physiol. (London)* **232**, 331–356.
2. Maren, S. & Baudry, M., *J. Cog. Neurosci.*, in press.
3. Baudry, M. & Davis, J. L., eds. (1991) *Long-Term Potentiation: A Debate of Current Issues* (MIT Press, Cambridge, MA).
4. Ambros-Ingersen, J., Larson, J., Xiao, P. & Lynch, G. (1991) *Synapse* **9**, 314–316.
5. Staubli, U., Kessler, M. & Lynch, G. (1990) *Psychobiology* **18**, 377–381.
6. Davies, S. N., Lester, R. A. J., Reymann, K. G. & Collingridge, G. L. (1989) *Nature (London)* **338**, 500–503.
7. Shahi, K. & Baudry, M. (1992) *Proc. Natl. Acad. Sci. USA* **89**, 6881–6885.
8. Manabe, T., Renner, P. & Nicoll, R. A. (1992) *Nature (London)* **355**, 50–55.
9. Maren, S., Baudry, M. & Thompson, R. F. (1992) *Synapse* **11**, 221–228.
10. Tocco, G., Maren, S., Shors, T. J., Baudry, M. & Thompson, R. F. (1992) *Brain Res.* **573**, 228–234.
11. Morris, R. G. M., Anderson, E., Lynch, G. S. & Baudry, M. (1986) *Nature (London)* **319**, 774–776.
12. Yeckel, M. F. & Berger, T. W. (1992) *Soc. Neurosci. Abstr.* **18**, 1494.
13. Nielsen, E. O., Drejer, J., Cha, J. J.-H., Young, A. B. & Honore, T. (1990) *J. Neurochem.* **54**, 686–695.
14. Massicotte, G., Bernard, J. & Baudry, M. (1992) *Dev. Brain Res.* **66**, 203–208.
15. Yeckel, M. F. & Berger, T. W. (1990) *Proc. Natl. Acad. Sci. USA* **87**, 5832–5836.
16. Berger, T. W. & Yeckel, M. F. (1991) in *Long-Term Potentiation: A Debate of Current Issues*, eds. Baudry, M. & Davis, J. L. (MIT Press, Cambridge, MA), pp. 327–356.
17. Hall, R., Kessler, M. & Lynch, G. (1992) *J. Neurochem.* **59**, 1997–2004.
18. Rao, G., Maren, S., Tocco, G., Baudry, M., Thompson, R. F., McNaughton, B. L. & Barnes, C. A. (1992) *Soc. Neurosci. Abstr.* **18**, 1215.